AIP | The Journal of Chemical Physics

Strong-field ionization rates of linear polyenes simulated with time-dependent configuration interaction with an absorbing potential

Pascal Krause and H. Bernhard Schlegel

Citation: The Journal of Chemical Physics **141**, 174104 (2014); doi: 10.1063/1.4900576
View online: http://dx.doi.org/10.1063/1.4900576
View Table of Contents: http://scitation.aip.org/content/aip/journal/jcp/141/17?ver=pdfcov
Published by the AIP Publishing

Strong-field ionization rates of linear polyenes simulated with time-dependent configuration interaction with an absorbing potential

Pascal Krause and H. Bernhard Schlegel
Department of Chemistry, Wayne State University, Detroit, Michigan 48202-3489, USA

(Received 8 August 2014; accepted 16 October 2014; published online 3 November 2014)

The strong field ionization rates for ethylene, trans 1,3-butadiene, and trans,trans 1,3,5-hexatriene have been calculated using time-dependent configuration interaction with single excitations and a complex absorbing potential (TDCIS-CAP). The calculations used the aug-cc-pVTZ basis set with a large set of diffuse functions (3 *s*, 2 *p*, 3 *d*, and 1 *f*) on each atom. The absorbing boundary was placed 3.5 times the van der Waals radius from each atom. The simulations employed a seven-cycle cosine squared pulse with a wavelength of 800 nm. Ionization rates were calculated for intensities ranging from 0.3×10^{14} W/cm^2 to 3.5×10^{14} W/cm^2. Ionization rates along the molecular axis increased markedly with increasing conjugation length. By contrast, ionization rates perpendicular to the molecular axis were almost independent of the conjugation length. © *2014 AIP Publishing LLC*. [http://dx.doi.org/10.1063/1.4900576]

I. INTRODUCTION

When molecules are exposed to short, intense laser pulses they can display various nonlinear optical phenomena (see, e.g., Refs. 1–3). One of the effects that can occur in ultrashort pulses with intensities in the $10^{13} - 10^{15}$ W/cm^2 range is strong field ionization (for leading references, see Refs. 4–28 and references therein). At these field strengths, electrons can be extracted directly out of bound states. Perturbative models cannot readily describe the electronic effects induced by such short, intense laser pulses. Methods which explicitly solve the time-dependent Schrödinger equation (TDSE) for electronic wavefunctions need to be employed. These time-dependent methods take into account the actual shape and phase of the laser pulses and can give further insight into the electron dynamics on their natural time scale, atto- and femto-seconds.

Highly accurate 3D simulations of the TDSE can be carried out for one and two electron systems using grid-based methods and basis set expansion approaches.[29–35] For larger many-electron systems, time-dependent Hartree-Fock (TDHF)[36] and time-dependent density functional theory (TDDFT)[37] can be used. For molecular calculations, atom-centered basis functions are often employed instead of grid-based or plane-wave methods. Computationally more demanding time-dependent wavefunction methods can treat electron correlation to different degrees. These include time-dependent configuration interaction (TDCI),[38–41] time-dependent coupled cluster (TDCC),[42,43] and multiconfiguration time-dependent Hartree-Fock (MCTDHF).[44–54] These simulations typically need large excited state manifolds and basis sets with multiple diffuse functions to describe the interaction with the laser field.[55–57]

TDCI simulations have been used to study the dynamics of bound electrons in state-to-state excitations[58–60] and charge migration occurring after ionization.[61–64] However, it is more difficult to carry out direct simulations of the ionization process since it produces an unbound electron. Grid and plane-wave methods can handle unbound electrons easily,[65,66] but it is more difficult to treat ionization with atom-centered basis sets. Complex excitation energies have been used with TDDFT[67] and TDCI[68] calculations to model the loss of electron density during ionization. Uhlmann *et al.*[67] assumed that all DFT states above the ionization potential are absorbing. In Klamroth's heuristic model,[68] orbital energies and an escape distance are used to estimate the lifetimes of CI states. We have used TDCIS and Klamroth's heuristic model to study the strong field ionization of linear polyenes.[69] Luppi and Head-Gordon[57] calculated high energy Rydberg states and the high-order harmonics spectrum of the hydrogen atom using Klamroth's heuristic model and a very large basis sets augmented with numerous diffuse shells and off-centered functions. A more detailed method for estimating the lifetime of CI states is to compute the integrals with a real-space complex absorbing potential (CAP). In a recent study,[70] we used TDCI with a CAP to examine strong field ionization of some many-electron polyatomic systems. Using a large atom-centered basis set augmented with numerous diffuse functions, we were able to see enhanced ionization rates for HCl^+ and HCO^+ as the bond lengths were stretched.

For a series of polyacenes, Dewitt and Levis showed that ionization rates depend dramatically on molecular length and conjugation.[71–73] Single active electron models such as ADK and molecular-ADK[74,75] did not give the correct ionization rates for these molecules. However, a structure-based model that incorporated both the ionization potential and electronic delocalization within the molecule, was able to correctly predict the relative rates for strong field ionization of benzene, naphthalene, and anthracene.[71–73] Suzuki and Mukamel have simulated the π electron dynamics and ionization in 1D models of octatetraene.[76,77] Corkum and co-workers have measured the ionization saturation intensities for a series organic molecules including ethylene and hexatriene.[78,79] Stolow and co-workers have studied the strong-field ionization of trans-butadiene, identifying the main channels in a time-resolved

fashion[23] and obtained channel- and angle-resolved ionization rates.[28] They found a strong angular dependence of the ionization rate, which agreed well with time-dependent resolution-in-ionic-states (TDRIS)[17] calculations but not with molecular ADK theory.[74,75]

In prior work, we have studied the electronic optical response of butadiene in short, intense laser pulses using TDHF, TDCIS, TDCIS(D), and TD-EOMCC.[40,56,80] In a recent study,[69] we have used TDCIS and Klamroth's heuristic model for ionization[68] to compare the strong field ionization rates of linear polyenes. In the present work, we employ our more accurate TDCIS-CAP approach[70] to simulate the interaction of short, intense laser pulses with a series of linear polyenes: ethylene, trans-butadiene, and all-trans-hexatriene. We discuss the ionization as a function of the intensity and orientation of the linearly polarized laser field and examine the dependence of the ionization rate on the conjugation length.

II. METHOD

Time-resolved electron dynamics is governed by solving the time-dependent Schrödinger equation for electronic wavefunctions:

$$\mathrm{i}\frac{\partial}{\partial t}\Psi_{\mathrm{el}}(t) = \hat{\mathbf{H}}(t)\Psi_{\mathrm{el}}(t). \tag{1}$$

To describe the interaction of the electrons with a laser source and with an absorbing potential, the total Hamilton operator has the form:

$$\hat{\mathbf{H}}(t) = \hat{\mathbf{H}}_{\mathrm{el}} - \hat{\vec{\boldsymbol{\mu}}}\vec{E}(t) - \mathrm{i}\hat{\mathbf{V}}^{\mathrm{Absorb}}, \tag{2}$$

where $\hat{\mathbf{H}}_{\mathrm{el}}$ is the usual field-free electronic Hamiltonian. The electron-light interaction is treated in the semi-classical dipole approximation, where $\hat{\vec{\boldsymbol{\mu}}}$ is the dipole operator and $\vec{E}(t)$ is the electric field component of the laser pulse. In this work, we apply linearly polarized cosine square shaped pulses as shown in Fig. 1(b):

$$\vec{E}(t) = \vec{s}(t)\cos\left[\omega t - \phi\right] \tag{3}$$

$$\vec{s}(t) = \begin{cases} \vec{E}_0 \cos^2\left(\frac{\pi}{2\sigma}t\right) & \text{for } -\sigma < t < \sigma \\ \vec{0} & \text{else}, \end{cases} \tag{4}$$

where ϕ denotes the phase and 2σ is the full duration of the pulse.

In Eq. (2), $-\mathrm{i}\hat{\mathbf{V}}^{\mathrm{Absorb}}$ is the complex absorbing potential (CAP). The CAP is constructed from a set of overlapping spherical potentials around each atom. Each spherical potential has a quadratic rise with curvature of 0.21, starting at r_a, and a quadratic fall-off until $V_{\max} = 10\ \mathrm{E_h}$ is reached. To model ionization by tunneling or barrier suppression, the CAP is placed outside of the Coulomb barrier but within the maximum excursion of the electron in the laser field ($\alpha = E_0/\omega^2 = 18.5\ \mathrm{a_0}$ for $E_0 = 0.06\ \mathrm{E_h/(ea_0)}$ and $\omega = 0.057\ \mathrm{E_h}/\hbar$). For hydrogen atoms $r_a = 9.524\ \mathrm{a_0}$ and for carbon atoms $r_a = 12.735\ \mathrm{a_0}$, which is 3.5 times the van der Waals radius of each element. In regions where these spheres overlap, the minimum value of the spherical potentials is used for the CAP. The chosen radii for the CAP are not sufficiently large to simulate high-order harmonics up to the cut-off region. They are a compromise between minimal norm absorption in the field-free case, stability of the ionization rates and the number of diffuse basis functions needed for interaction with the CAP.

To solve Eq. (1), the time-dependent wavefunction is expressed in the basis of ground and excited states of the field-free, time-independent Hamiltonian, $\hat{\mathbf{H}}_{\mathrm{el}}|\Psi_i\rangle = \omega_i|\Psi_i\rangle$:

$$\Psi(t) = \sum_{i=0} C_i(t)|\Psi_i\rangle, \tag{5}$$

which leads to a set of coupled differential equations for the coefficients:

$$\mathrm{i}\frac{\partial}{\partial t}C_i(t) = \sum_j \left\langle \Psi_i \left| \hat{\mathbf{H}}(t) \right| \Psi_j \right\rangle C_j(t). \tag{6}$$

A unitary transformation at the midpoint of the time step gives the numerical evolution of the coefficients:

$$\vec{C}(t + \Delta t) = \exp\left[-\mathrm{i}\mathbf{H}(t + \Delta t/2)\Delta t\right]\vec{C}(t). \tag{7}$$

The GAUSSIAN program package[81] was used to obtain the field-free configuration interaction singles (CIS)[82] wavefunctions. Although the longer polyenes have some low lying doubly excited states,[83] their effect on the single ionization rate should be small since one-photon transitions from the ground state to doubly excited states are forbidden. The time-dependent configuration interaction singles (TDCIS) propagations in this work have been carried out using a time step of $\Delta t = 0.05\ \hbar/\mathrm{E_h}$(1.2 as) and a total propagation time of 1000 $\hbar/\mathrm{E_h}$(24.2 fs). In previous tests,[70] reducing the time step from $\Delta t = 0.05\ \hbar/\mathrm{E_h}$ to $\Delta t = 0.025\ \hbar/\mathrm{E_h}$ changed the norm at the end of an intense pulse with a field strength of 0.09 $\mathrm{E_h/(ea_0)}$ by less than 0.02%.

The standard Dunning aug-cc-pVTZ basis set[84,85] was employed for each atom together with the absorbing basis set used in an earlier publication.[70] The aug-cc-pVTZ basis adequately describes the valence space of the molecule (up to ~5 $\mathrm{a_0}$). The Gaussian functions of the absorbing basis are chosen to span the rest of the space out to the CAP and have half widths at half maximum of 5-10 $\mathrm{a_0}$. Absorbing basis 1 (AB1) is our default absorbing basis set and it is constructed of three *s* type Gaussian functions with exponents 0.0256, 0.0128, and 0.0064, two *p* functions with exponents 0.0256 and 0.0128, three *d* functions with exponents 0.0512, 0.0256, and 0.0128, and one *f* type Gaussian function with exponent 0.0256. We carried out basis set tests and extended and/or reduced the default AB1 as follows. AB2 contains an additional *p* type Gaussian function with exponent 0.0064 on the C atom. For AB3, we have added an additional *s* type function (with exponent 0.0032) and two *p* type functions (with exponent 0.0064 and 0.0032) to AB1 on the C atom. For AB4, we removed the *f* type Gaussian function for the hydrogen atoms from AB1. AB5 contains no *f* type functions for the hydrogen atoms but has an additional *p* type function with exponent 0.0064 on the C atom with respect to AB1.

TABLE I. Static properties of the three polyenes (HF/6-31G(d,p) for the bond lengths given in Å, aug-cc-pVTZ+AB1 for the ground and first excited state energies and vertical ionization potentials in E_h).

	R(C-H)	R(C-C)	R(C=C)	E_0(RHF)	E_1(CIS)	I_p
Ethylene	1.0766	...	1.3168	− 78.065297	− 77.799429	0.3306
Butadiene	1.0751, 1.0772, 1.0788	1.4670	1.3222	− 154.980287	− 154.749640	0.2826
Hexatriene	1.0748, 1.0770, 1.0794	1.4629	1.3234, 1.3289	− 231.895752	− 231.689659	0.2540

III. RESULTS

As in the previous study, the HF/6-31G(d,p) optimized geometries were used for ethylene, butadiene, and hexatriene. Table I summarizes the bond lengths; these are within 0.003 Å of the HF/aug-cc-pVTZ values. The HF/6-31G(d,p) geometries were used for the CIS calculations which employed the aug-cc-pVTZ basis set[84,85] together with the absorbing basis AB1. The CIS calculations give 1849 electronic states for ethylene, 5468 states for butadiene, and 10897 states for hexatriene.

Table I lists the energies of ground and first excited state with the aug-cc-pVTZ+AB1 basis. Also shown are vertical ionization potentials, I_p, calculated by ΔSCF. The ionization potentials decrease with the length of the conjugated π system of the polyene, and the ionization rates are be expected to increase, as will be seen below.

The ionization rates presented in the following are obtained by a cosine squared pulse and have been estimated from the loss of norm divided by the pulse duration:

$$\Gamma_{\text{ion}} = (1 - n(t_{\text{end}}))/2\sigma, \tag{8}$$

where $n(t_{\text{end}})$ is the norm of the wavefunction at the end of the pulse and $2\sigma = 18.7$ fs is the full duration of a seven-cycles pulse with a frequency of $\hbar\omega = 0.057$ E_h(800 nm).

A. Polyenes in an intense laser pulse

The orientation of the polyenes in the laser pulse is shown in Fig. 1(a). The molecular axis is taken as the vector between the first and last carbon atom. The two orthogonal axes are in the plane and perpendicular to the molecular plane. The time-dependent electric field of the cosine squared pulse with the maximal field strength of $E_0 = 0.05$ $E_h/(ea_0)$ (0.88×10^{14} W/cm^2) is plotted in Fig. 1(b). The progression of the norm for ethylene (blue), butadiene (green), and hexatriene (red), respectively, are shown in Fig. 1(c) for a linearly polarized pulse aligned with the molecular axis.

The norms of the polyenes decay at significantly different rates. As a result of the applied field, electron density is distorted from its equilibrium distribution towards the CAP. Interaction with the CAP causes the norm of the wavefunction to decrease which, in turn, is interpreted as the ionization process. The decaying norm shows oscillations which correlate with the oscillations of the field; at the zero-crossings of the field, the norm decay reaches a plateau. The oscillations in the norm reflect the change in the single ionization rate as a function of the field strength rather than steps in multiple ionizations. To treat multiple ionizations, the TDCI calculations would need to include multiple excitations rather than only single excitations.

Figure 1(c) shows that the norm of ethylene barely decreases, dropping only to 0.977 after the pulse, i.e., almost no ionization has taken place. With the same pulse, hexatriene ionizes much easier with its norm decreasing to 0.370. An intermediate loss of norm (0.757) is observed for butadiene. As mentioned above, such behaviour is expected from the ionization potentials—the smaller the ionization potential, the lower the Coulombic barrier for ionization. Tunneling through the barrier can be described by ADK theory[74,75] and is proportional to $\exp(-2\kappa^3/3E_0)$ where $\kappa^2/2 = I_p$. Strong field ionization may also correlate with the molecular polarizability. The electron density can be distorted more easily along directions of greater polarizability. The laser field could push more electron density toward the Coulomb barrier and thereby increase the ionization rate. The experimental polarizabilities, $\bar{\alpha}$, are 28.70 a_0^3 for ethylene[86] and 54.64 a_0^3 for butadiene,[87] and 87.46 for hexatriene.[88] The polarizabilities computed with the aug-cc-pVTZ+AB1 basis are listed in Table II. Note that the polarizability along the molecular axis, α_{xx}, grows more rapidly than the isotropic polarizability, $\bar{\alpha}$.

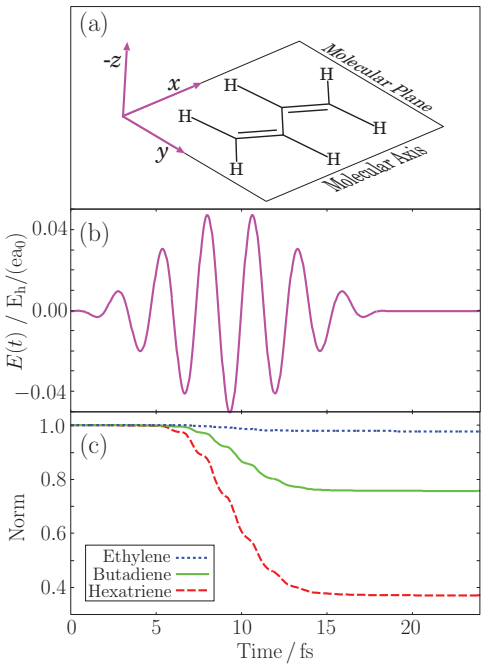

FIG. 1. (a) Molecular orientation for butadiene. The molecular axis is the vector through the first and last carbon atom of the polyenes. (b) Electric field for a seven-cycle cosine squared pulse with a field strength of $E_0 = 0.05$ $E_h/(ea_0)$ and a frequency of $\hbar\omega = 0.057$ E_h. (c) Progressions of the wavefunction norm during the laser pulse for ethylene (blue, dotted), butadiene (green solid), and hexatriene (red, dashed) employing the aug-cc-pVTZ+AB1 basis.

TABLE II. Static polarizabilities (diagonal elements in a_0^3) (see Fig. 1(a) for the orientation).

	RHF: $(\alpha_{xx}, \alpha_{yy}, \alpha_{zz}), \bar{\alpha}$
Ethylene	(35.815, 24.216, 22.460), 27.497
Butadiene	(85.655, 43.858, 36.8227), 55.445
Hexatriene	(157.165, 62.8971, 50.7566), 90.27

In an earlier study, we used Klamroth's heuristic model to approximate the ionization rates for polyenes[69] using the 6-31G(d,p) basis set augmented with 3 sets of diffuse sp functions on each carbon. Compared to the absorbing potential approach, the loss in norm is generally larger using the heuristic model, since all states above the I_p in this methodology are ionizing. With the present method, only orbitals that interact with the absorbing potential lead to loss of electron density. Not only this is a more physical model, but it also allows for different ionization rates depending on the orientation of the molecule in the laser field.

B. Basis set tests

The original absorbing basis was developed for the hydrogen atom and tested extensively as described previously.[70] Because the polyenes have extended π systems, further tests of the absorbing basis are needed. As above described, we have constructed a series of absorbing basis sets with additional *s* and *p* type function on the C atom and/or removed *f* type function on the H atoms. In Fig. 2, the tests with the five different absorbing basis set are shown for ethylene and butadiene for various field strengths. With the largest set, AB3, the CIS calculations give 1909 states for ethylene, and 5677 states in butadiene, while the smallest set, AB4, leads to 1735 and 5248 states, respectively.

Figure 2 shows the ionization rates for seven-cycle cosine squared pulses with a frequency of $\hbar\omega = 0.057$ E_h and field strengths ranging from 0.03 to 0.10 $E_h/(ea_0)$. Naturally, with increasing field strength there is a large increase in the ionization rate (discussed in more detail in Sec. III D). The differences in the ionization rate with changes in the basis set, however, are rather small for any field strength. The only significant effect is for ethylene when *f* function on the hydrogen atoms are removed from the basis set (AB4 (pink) and AB5 (cyan)). For the field strength of 0.07 through 0.09 $E_h/(ea_0)$, the rates are slightly smaller. Such differences with the basis set, however, disappear almost completely for butadiene. Propagations for hexatriene with the AB1 and AB4 resulted in virtually the same ionization rates (not shown). Additional *s* and *p* functions (AB2 (red) and AB3 (green)) seem to have no impact. Since extending the basis set beyond AB1 does not change the ionization rate significantly, AB1 will be used for the further simulations.

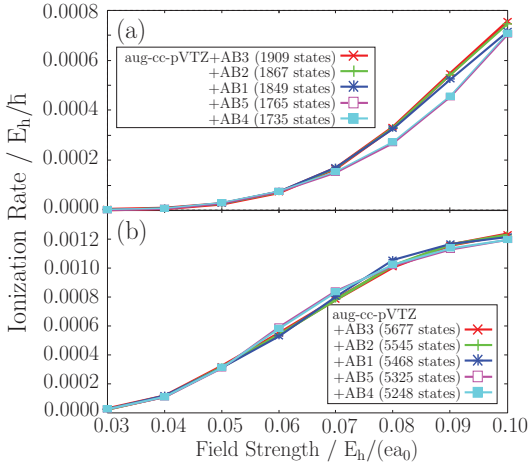

FIG. 2. Basis set tests for ethylene (top panel) and butadiene (bottom panel) employing the aug-cc-pVTZ plus absorbing basis 1 through 5 (see text). Ionization rate as a function of field strength of a seven-cycle cosine squared pulse with a frequency of $\hbar\omega = 0.057$ E_h and aligned with the molecular axis.

C. Reducing the number of excited states

To examine the contribution of high-lying excited states, we carried out simulations with successively decreasing numbers of electronic states. Figure 3 shows the ionization rates as a function of the energy of the highest excited state included in the TDCIS propagation. For better comparison between the polyenes, Fig. 3(b) shows the difference in the rates as a function of the highest energy state included ($\Delta\Gamma_{ion} = \Gamma_{ion}(E) - \Gamma_{ion}(E_{max})$). One can see that states higher than 2 E_h(54.42 eV) do not significantly contribute to the ionization rate. For ethylene, only about 1300 out of 1849 states are needed to obtain the same change in the norm, for butadiene 3500 out of 5468 states are enough, and for hexatriene 7000 out of 10 897 states are sufficient. Roughly two-thirds of the singly excited state mainfold is required to reproduce the same ionization rates with the present basis set and absorbing potential.

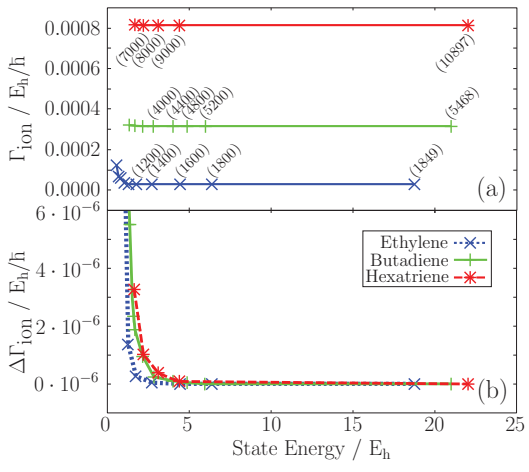

FIG. 3. Comparison of ionization rates as a function of highest energy of states included. The plot shows, with a reduced number of states, (a) the ionization rates, and (b) the difference to the rate with the full set of states. The aug-cc-pVTZ+AB1 basis set was employed for all polyenes. A seven-cycle cosine squared pulse with a frequency of $\hbar\omega = 0.057$ E_h and a field strength of $E_0 = 0.05$ $E_h/(ea_0)$ was aligned with the molecular axis. The number of states included in the simulations is indicated at the points on the curve.

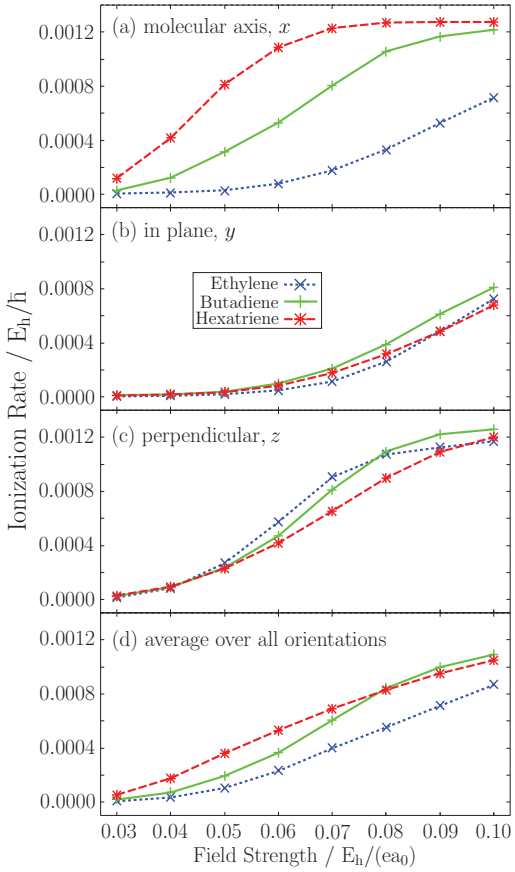

FIG. 4. Comparison of ionization rates as a function of applied field strength and laser field orientation (see Fig. 1(a) for orientations): (a) molecular axis, (b) in plane, and (c) perpendicular. Ionization was with a seven-cycle cosine squared pulse with a frequency of $\hbar\omega = 0.057$ E_h. The aug-cc-pVTZ+AB1 basis set was employed and the full set of states (1849, 5468, and 10897 states) was used in the propagation.

D. Laser field orientation

The ionization rates are shown in Fig. 4 as a function of applied field strength for orientations along the molecular axis and in perpendicular directions. Generally, the rates reach a plateau at high field strengths. This is because the rates are approximated by the total decrease in the norm of the wavefunction. At high field strengths, the norm can reach zero before the pulse has ended, thereby limiting the maximum rate.

When the laser field is directed along the molecular axis (Fig. 4(a)) the ionization rates of polyenes differ the most. Ethylene has the lowest rates for all field strengths, butadiene is intermediate, and hexatriene has the highest ionization rates for all field strengths. This is as expected from the ionization potentials. The highest occupied orbitals are the π orbitals and their energy changes the most as the conjugation length increases. With the laser field applied along the molecular axis, the highest π orbital will be the largest contributor to the ionization. The ionization rates also follow the trends in the polarizabilities, particularly α_{xx} which is in the direction of the molecular axis. The wavefunction can be distorted more easily by a field in this direction, and thus can more readily reach the absorbing boundary.

The same general trends and shapes of the ionization curves along the molecular axis were found in our earlier work using the heuristic model for ionization.[68] A more quantitative way of comparing the results is to examine the field strengths required to produce a specific decrease in the norm of the wavefunction. With the present TDCIS-CAP method, field strengths of 0.096, 0.064, and 0.046 $E_h/(ea_0)$ are required for a 50% decrease in the norm for ethylene, butadiene, and hexatriene, respectively. This can be compared to the heuristic approach for which the field strengths are 0.037, 0.029, and 0.025 $E_h/(ea_0)$ (a 50% decrease in norm corresponds to a 75% decrease in the population).[69] The field strengths required for the heuristic approach are much smaller because essentially all of the states above the ionization potential are absorbing.

Ionization rates for laser polarizations perpendicular to the molecular axis in the molecular plane and perpendicular to it are shown in Figs. 4(b) and 4(c). In contrast to the laser field along the molecular axis, the rates for the two other directions differ only a little between the polyenes. For the field in the molecular plane (Fig. 4(b)), we observe the same low rates for all polyenes. This is most likely due to the fact that the laser field is oriented along the carbon-hydrogen σ bonds. The electrons in the σ bonds are more tightly bound than those in the π bonds, and thus do not contribute as much to the ionization process. The rates are significantly higher when the laser field is perpendicular to the molecular plane (Fig. 4(c)) because the ionization comes from the more weakly bound electrons in the π orbitals. With the field perpendicular to the molecular plane, these electrons can ionize directly similar to atomic p orbitals and there is little difference between the three polyenes. By contrast, for the laser field along the molecular axis, the increasing length of the conjugated π system allows for considerably more dynamics of the electrons and a greater difference in the ionization rates.

Direct comparison of the ionization rates can be difficult because of differences in intensity, pulse shape, and duration, and differences in the quantities calculated or measured. Some of these difficulties can be circumvented by examining the ratios of intensities or field strengths. Relative to ethylene, the ratios of the field strengths required to produce a 50% decrease in the wavefunction norm are 1, 0.66, and 0.48 for ethylene, butadiene, and hexatriene for ionization along the molecular axis calculated with the TDCIS-CAP method. For the heuristic approach, the ratios are 1, 0.78, and 0.67, respectively. The decrease in the ratio going from ethylene to hexatriene is much smaller in the heuristic case, probably because it does not treat the directionality of the ionization adequately. Corkum and co-workers[78,79] have measured ionization saturation intensities for a number of hydrocarbons. They obtained $I_{sat} = 1.10 \times 10^{14}$ W/cm^2 for ethylene and $I_{sat} = 0.89 \times 10^{14}$ W/cm^2 for hexatriene. To compare with the ratio of measured saturation intensities, the calculations must be averaged over orientation. The calculated ionization rates averaged over the x, y, and z directions are shown in Fig. 4(d). The ratios of the field strengths required to produce a 50% decrease in the wavefunction norm are 1, 0.84, and 0.78 for ethylene, butadiene, and hexatriene. The corresponding ratio of calculated intensities for hexatriene vs. ethylene, $0.78^2 = 0.61$, is significantly smaller than the ratio of the measured

ionization saturation intensities, 0.81. Possible contributors to this difference are concerns of molecular conformations and partial alignment in the experimental measurements and details of the angular dependence do not capture by a simple average over the 3 axes in the calculations.

Angular distributions of strong field ionization probabilities have been obtained for a number of simple molecules.[89–91] Recently, Stolow and co-workers[28] have measured the channel- and angle-resolved above threshold ionization probabilities for butadiene. They found that ionization is maximal along the principal axis and lower in perpendicular directions. Time-dependent resolution-in-ionic-states (TDRIS)[17] simulations agreed with the measurements better than molecular ADK[74,75] calculations. Our TDCIS-CAP calculations also show a large difference in the angular ionization rates favoring the molecular axis over perpendicular directions, especially for butadiene and hexatriene. These calculations show as well that this difference decreases as the intensity increases.

IV. SUMMARY

The TDCIS-CAP method makes it possible to simulate ionization processes for polyatomic molecules. In this study, we examined the trends in strong field ionization rates for a set of linear polyenes: ethylene, butadiene, and hexatriene. The simulations used 800 nm 7 cycle cosine squared pulses with intensities ranging from 0.3×10^{14} W/cm^2 to 3.5×10^{14} W/cm^2. For a given intensity, the ionization rates along the molecular axis increased dramatically with increasing π system length. The calculations used an aug-cc-pVTZ basis supplemented by a large set of diffuse functions (3 *s*, 2 *p*, 3 *d*, and 1 *f*) on each atom. Tests with additional diffuse functions showed that this basis set was satisfactory for calculating the ionization rates for these molecules. Such large basis sets generate an even larger number of singly excited states. Using a maximum energy cut-off, we found that only about two-third of the excited state manifold was needed to produce the same ionization rate. The laser field was oriented along the molecular axis (first carbon to last carbon) or perpendicular to it, either in the molecular plane or perpendicular to it. For the laser field along the molecular axis, the rates depend strongly on the length of the conjugated system. Compared to ethylene, hexatriene required only a quarter of the laser intensity to achieve the same amount of ionization along the molecular axis. In contrast, for the two directions perpendicular to the molecular axis, the ionization rate did not depend significantly on the conjugation length. Our next step will be to use the present methodology to map out the angular dependence of the ionization rates for the polyenes and compare them with recent experimental data for butadiene.[28] We will also explore the relative contribution of the higher lying valence orbitals to the ionization rate as a function of the laser intensity.

ACKNOWLEDGMENTS

This work was supported by a grant from the National Science Foundation (CHE1212281). We thank Wayne State University's computing grid for computer time.

[1] *Strong Field Laser Physics*, Springer Series in Chemical Physics Vol. 134, edited by T. Brabec (Springer, New York, 2009).
[2] H. Reiss in *Lectures on Ultrafast Intense Laser Science 1*, Springer Series in Chemical Physics Vol. 94, edited by K. Yamanouchi (Springer, Berlin/Heidelberg, 2011), pp. 41–84.
[3] F. Krausz and M. Ivanov, Rev. Mod. Phys. **81**, 163 (2009).
[4] T. Brabec and F. Krausz, Rev. Mod. Phys. **72**, 545 (2000).
[5] W. Becker, F. Grasbon, R. Kopold, D. Milošević, G. Paulus, and H. Walther, Adv. At., Mol., Opt. Phys. **48**, 35 (2002).
[6] F. Grasbon, G. G. Paulus, H. Walther, P. Villoresi, G. Sansone, S. Stagira, M. Nisoli, and S. De Silvestri, Phys. Rev. Lett. **91**, 173003 (2003).
[7] P. Agostini and L. F. DiMauro, Rep. Prog. Phys. **67**, 813 (2004).
[8] M. Y. Ivanov, M. Spanner, and O. Smirnova, J. Mod. Opt. **52**, 165 (2005).
[9] D. B. Milošević, G. G. Paulus, D. Bauer, and W. Becker, J. Phys. B: At., Mol. Opt. Phys. **39**, R203 (2006).
[10] O. Smirnova, M. Spanner, and M. Ivanov, J. Mod. Opt. **54**, 1019 (2007).
[11] M. Vrakking, in *Progress in Ultrafast Intense Laser Science II*, Springer Series in Chemical Physics Vol. 85 (Springer, Berlin/Heidelberg, 2007), pp. 43–63.
[12] M. F. Kling and M. J. Vrakking, Annu. Rev. Phys. Chem. **59**, 463 (2008).
[13] H. R. Reiss, in *Progress in Ultrafast Intense Laser Science III*, Springer Series in Chemical Physics Vol. 89 (Springer, Berlin/Heidelberg, 2008), pp. 1–31.
[14] M. Awasthi, Y. V. Vanne, A. Saenz, A. Castro, and P. Decleva, Phys. Rev. A **77**, 063403 (2008).
[15] C. I. Blaga, F. Catoire, P. Colosimo, G. G. Paulus, H. G. Muller, P. Agostini, and L. F. DiMauro, Nat. Phys. **5**, 335 (2009).
[16] G. Paulus, in *Progress in Ultrafast Intense Laser Science*, Springer Series in Chemical Physics Vol. 91, edited by K. Yamanouchi, A. Becker, R. Li, and S. Chin (Springer, Berlin/Heidelberg, 2009), pp. 17–40.
[17] M. Spanner and S. Patchkovskii, Phys. Rev. A **80**, 063411 (2009).
[18] Z. H. Goulielmakis, Z. H. Loh, A. Wirth, R. Santra, N. Rohringer, V. S. Yakovlev, S. Zherebtsov, T. Pfeifer, A. M. Azzeer, M. F. Kling *et al.*, Nature (London) **466**, 739 (2010).
[19] H. Kono in *Lectures on Ultrafast Intense Laser Science 1*, Springer Series in Chemical Physics Vol. 94, edited by K. Yamanouchi (Springer, Berlin/Heidelberg, 2011), pp. 111–134.
[20] M. Wollenhaupt and T. Baumert, Faraday Discuss. **153**, 9 (2011).
[21] P. Agostini, and L. F. DiMauro, in *Advances in Atomic, Molecular, and Optical Physics*, Advances in Atomic, Molecular, and Optical Physics Vol. 61, edited by E. A. Paul Berman, and C. Lin (Academic Press, 2012), pp. 117–158.
[22] A. D. Bandrauk and F. Légaré, *Enhanced Ionization of Molecules in Intense Laser Fields* (Springer, Berlin/Heidelberg, 2012), Vol. 8, Chap. 2, pp. 29–46.
[23] A. E. Boguslavskiy, J. Mikosch, A. Gijsbertsen, M. Spanner, S. Patchkovskii, N. Gador, M. J. J. Vrakking, and A. Stolow, Science **335**, 1336 (2012).
[24] L. Gallmann, C. Cirelli, and U. Keller, Annu. Rev. Phys. Chem. **63**, 447 (2012).
[25] R. Boge, C. Cirelli, A. S. Landsman, S. Heuser, A. Ludwig, J. Maurer, M. Weger, L. Gallmann, and U. Keller, Phys. Rev. Lett. **111**, 103003 (2013).
[26] M. Hellgren, E. Räsänen, and E. K. U. Gross, Phys. Rev. A **88**, 013414 (2013).
[27] O. Njoya, S. Matsika, and T. Weinacht, ChemPhysChem **14**, 1451 (2013).
[28] J. Mikosch, A. E. Boguslavskiy, I. Wilkinson, M. Spanner, S. Patchkovskii, and A. Stolow, Phys. Rev. Lett. **110**, 023004 (2013).
[29] A. Picón, A. Jaroń-Becker, and A. Becker, Phys. Rev. Lett. **109**, 163002 (2012).
[30] M. R. Hermann and J. A. Fleck, Jr., Phys. Rev. A **38**, 6000 (1988).
[31] M. Hehenberger, H. V. McIntosh, and E. Brändas, Phys. Rev. A **10**, 1494 (1974).
[32] A. D. Bandrauk and H. Z. Lu, Phys. Rev. A **62**, 053406 (2000).
[33] T. K. Kjeldsen, L. B. Madsen, and J. P. Hansen, Phys. Rev. A **74**, 035402 (2006).
[34] K. Harumiya, H. Kono, Y. Fujimura, I. Kawata, and A. D. Bandrauk, Phys. Rev. A **66**, 043403 (2002).
[35] E. Dehghanian, A. D. Bandrauk, and G. L. Kamta, Phys. Rev. A **81**, 061403 (2010).
[36] K. C. Kulander, Phys. Rev. A **36**, 2726 (1987).
[37] E. Runge and E. K. U. Gross, Phys. Rev. Lett. **52**, 997 (1984).
[38] P. Krause, T. Klamroth, and P. Saalfrank, J. Chem. Phys. **123**, 074105 (2005).

[39]F. Remacle, R. Kienberger, F. Krausz, and R. D. Levine, Chem. Phys. **338**, 342 (2007).
[40]H. B. Schlegel, S. M. Smith, and X. Li, J. Chem. Phys. **126**, 244110 (2007).
[41]L. Greenman, P. J. Ho, E. Karmarchik, D. A. Mazzoni, and R. Santra, Phys. Rev. A **82**, 023406 (2010).
[42]C. Huber and T. Klamroth, J. Chem. Phys. **134**, 054113 (2011).
[43]S. Kvaal, J. Chem. Phys. **136**, 194109 (2012).
[44]F. Remacle, M. Nest, and R. D. Levine, Phys. Rev. Lett. **99**, 183902 (2007).
[45]T. Kato and H. Kono, J. Chem. Phys. **128**, 184102 (2008).
[46]T. Kato and H. Kono, Chem. Phys. **366**, 46 (2009).
[47]M. Nest, T. Klamroth, and P. Saalfrank, Z. Phys. Chem. **224**, 569 (2010).
[48]S. Sukiasyan, S. Patchkovskii, O. Smirnova, T. Brabec, and M. Y. Ivanov, Phys. Rev. A **82**, 043414 (2010).
[49]D. Hochstuhl and M. Bonitz, J. Chem. Phys. **134**, 084106 (2011).
[50]D. J. Haxton, K. V. Lawler, and C. W. McCurdy, Phys. Rev. A **86**, 013406 (2012).
[51]H. Miyagi and L. B. Madsen, Phys. Rev. A **87**, 062511 (2013).
[52]T. Sato and K. L. Ishikawa, Phys. Rev. A **88**, 023402 (2013).
[53]H. Miyagi and L. Bojer Madsen, J. Chem. Phys. **140**, 164309 (2014).
[54]H. Miyagi and L. B. Madsen, Phys. Rev. A **89**, 063416 (2014).
[55]P. Krause, T. Klamroth, and P. Saalfrank, J. Chem. Phys. **127**, 034107 (2007).
[56]J. A. Sonk, M. Caricato, and H. B. Schlegel, J. Phys. Chem. A **115**, 4678 (2011).
[57]E. Luppi and M. Head-Gordon, J. Chem. Phys. **139**, 164121 (2013).
[58]P. Krause, T. Klamroth, and P. Saalfrank, J. Chem. Phys. **128**, 234307 (2008).
[59]I. Barth, J. Manz, Y. Shigeta, and K. Yagi, J. Am. Chem. Soc. **128**, 7043 (2006).
[60]T. Klamroth, J. Chem. Phys. **124**, 144310 (2006).
[61]J. Breidbach and L. S. Cederbaum, J. Chem. Phys. **118**, 3983 (2003).
[62]J. Breidbach and L. S. Cederbaum, J. Chem. Phys. **126**, 034101 (2007).
[63]G. Periyasamy, R. D. Levine, and F. Remacle, Chem. Phys. **366**, 129 (2009).
[64]A. I. Kuleff and L. S. Cederbaum, J. Phys. B: At., Mol. Opt. Phys. **47**, 124002 (2014).
[65]B. Mignolet, R. D. Levine, and F. Remacle, Phys. Rev. A **86**, 053429 (2012).
[66]B. Mignolet, R. D. Levine, and F. Remacle, Phys. Rev. A **89**, 021403 (2014).
[67]M. Uhlmann, T. Kunert, and R. Schmidt, J. Phys. B: At., Mol. Opt. Phys. **39**, 2989 (2006).
[68]S. Klinkusch, P. Saalfrank, and T. Klamroth, J. Chem. Phys. **131**, 114304 (2009).
[69]J. A. Sonk and H. B. Schlegel, J. Phys. Chem. A **116**, 7161 (2012).
[70]P. Krause, J. Sonk, and H. B. Schlegel, J. Chem. Phys. **140**, 174113 (2014).
[71]M. J. DeWitt and R. J. Levis, Phys. Rev. Lett. **81**, 5101 (1998).
[72]M. J. DeWitt and R. J. Levis, J. Chem. Phys. **110**, 11368 (1999).
[73]R. J. Levis and M. J. DeWitt, J. Phys. Chem. A **103**, 6493 (1999).
[74]M. V. Ammosov, N. B. Delone, and V. P. Krainov, Sov. Zh. Eksp. Teor. Fiz. **91**, 2008 (1986) [Sov. Phys. JETP **64**, 1191 (1986)].
[75]X. M. Tong, Z. X. Zhao, and C. D. Lin, Phys. Rev. A **66**, 033402 (2002).
[76]M. Suzuki and S. Mukamel, J. Chem. Phys. **119**, 4722 (2003).
[77]M. Suzuki and S. Mukamel, J. Chem. Phys. **120**, 669 (2004).
[78]S. M. Hankin, D. M. Villeneuve, P. B. Corkum, and D. M. Rayner, Phys. Rev. Lett. **84**, 5082 (2000).
[79]S. M. Hankin, D. M. Villeneuve, P. B. Corkum, and D. M. Rayner, Phys. Rev. A **64**, 013405 (2001).
[80]S. M. Smith, X. Li, A. N. Markevitch, D. A. Romanov, R. J. Levis, and H. B. Schlegel, J. Phys. Chem. A **109**, 5176 (2005).
[81]M. J. Frisch, G. W. Trucks, H. B. Schlegel *et al.*, Gaussian Development Version, Revision H.20+, Gaussian, Inc., Wallingford, CT, 2010.
[82]J. B. Foresman, M. Head-Gordon, J. A. Pople, and M. J. Frisch, J. Phys. Chem. **96**, 135 (1992).
[83]J. H. Starcke, M. Wormit, J. Schirmer, and A. Dreuw, Chem. Phys. **329**, 39 (2006).
[84]T. H. Dunning, Jr., J. Chem. Phys. **90**, 1007 (1989).
[85]A. K. Wilson, T. van Mourik, and T. H. Dunning, Jr., J. Mol. Struct.: THEOCHEM **388**, 339 (1996).
[86]T. K. Bose and R. H. Cole, J. Chem. Phys. **54**, 3829 (1971).
[87]U. Hohm and U. Trumper, Ber. Bunsenges. Phys. Chem. **96**, 1061 (1992).
[88]C. Weast, *CRC Hand Book of Chemistry and Physics*, 66th ed. (CRC Press, Boca Raton, 1985–1986)
[89]H. Akagi, T. Otobe, A. Staudte, A. Shiner, F. Turner, R. Dörner, D. M. Villeneuve, and P. B. Corkum, Science **325**, 1364 (2009).
[90]A. S. Alnaser, S. Voss, X. M. Tong, C. M. Maharjan, P. Ranitovic, B. Ulrich, T. Osipov, B. Shan, Z. Chang, and C. L. Cocke, Phys. Rev. Lett. **93**, 113003 (2004).
[91]A. S. Alnaser, C. M. Maharjan, X. M. Tong, B. Ulrich, P. Ranitovic, B. Shan, Z. Chang, C. D. Lin, C. L. Cocke, and I. V. Litvinyuk, Phys. Rev. A **71**, 031403 (2005).